

Topic 2F - Valence Bond Theory

Theories of Chemical Bonding

Satisfactory theory of chemical bonding should explain:

- Bond lengths**
- Bond strengths**
- Bond polarities**
- Molecular geometries**
- Molecular Para- and Diamagnetism**

Molecular Orbital Model

- Linear Combination of Atomic Orbitals (LCAO)**
- Delocalized Electron Density**
- Differing Electron Energies**
- M.O. Types**
 - Bonding**
 - Anti-Bonding**

Valence-Bond Model

- Atomic Orbital Overlap**
- Electron-Pair Bonds**
- Localized Electron Density**
- Orbital "Hybridization"**
- Bond Types**
 - σ -Bonds**
 - π -Bonds**

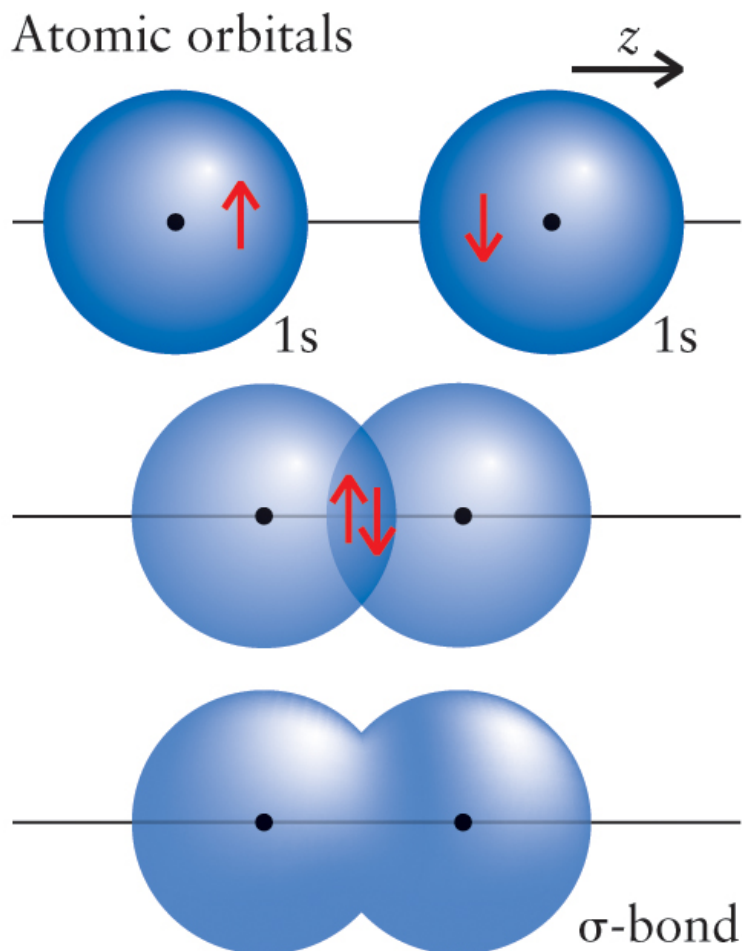


FIGURE 4.8 When electrons with opposite spins (depicted as \uparrow and \downarrow) in two hydrogen 1s-orbitals pair and the s-orbitals overlap, they form a σ -bond, which is depicted here by the boundary surface of the electron cloud. The cloud has cylindrical symmetry around the internuclear axis and spreads over both nuclei. In the illustrations in this book, σ -bonds are usually colored blue.

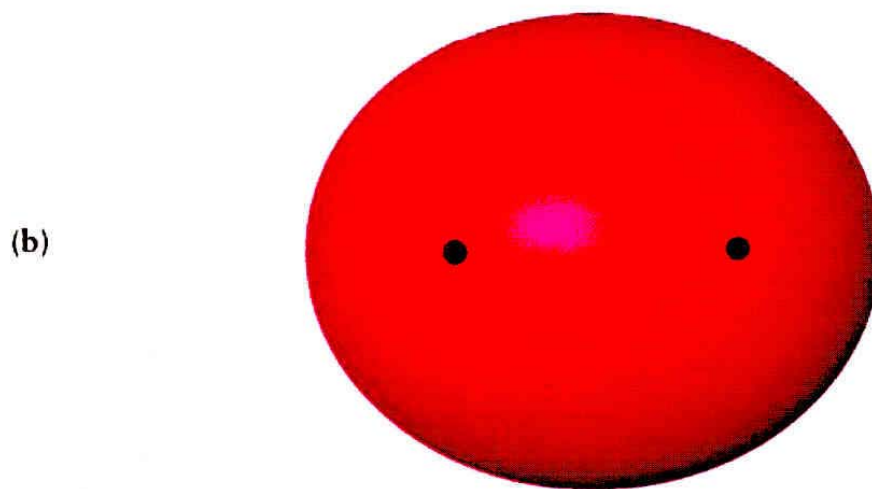
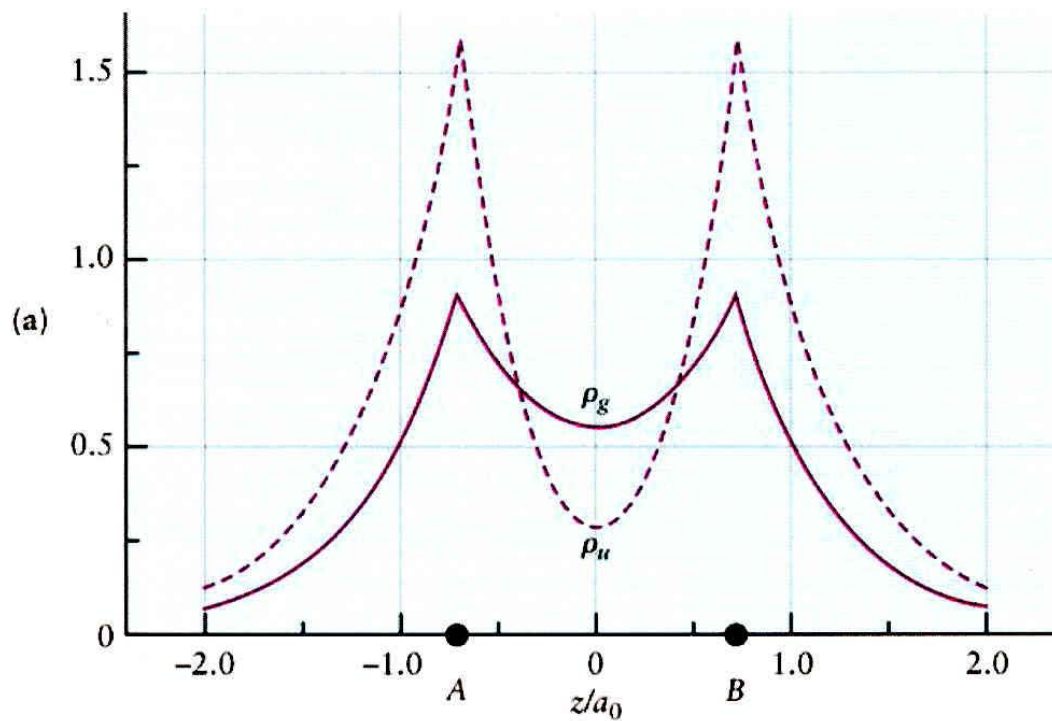
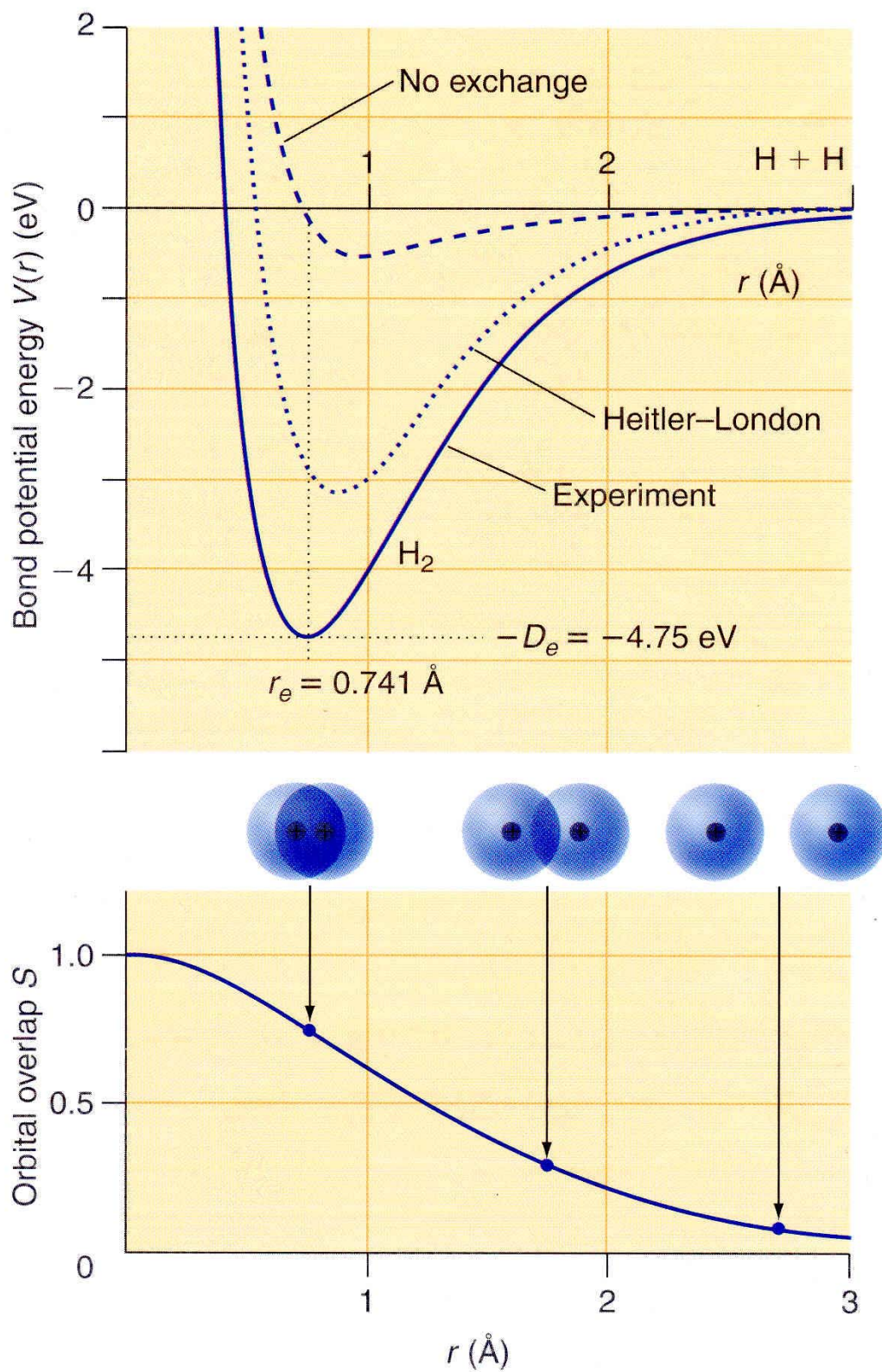


FIGURE 6.37 The electron density for the ψ_g^{el} and ψ_u^{el} wave functions in the simple valence bond model for H_2 . (a) The electron density ρ_g for ψ_g^{el} and ρ_u for ψ_u^{el} , calculated analytically as described in the text. (b) Three-dimensional isosurface of the electron density for the ψ_g^{el} wave function, as calculated numerically by Generalized Valence Bond Theory (GVB).

Figure 6.2: Bond Potential Energy Curves

Born-Oppenheimer Approximation

Assumes that, because nuclei in molecules are much more massive than electrons, the nuclear motions are negligibly slow compared to electronic motions. According to the Bohr model, for example, the velocity of an electron in the ground state of a hydrogen atom is given by:

$$v_{\text{el}} = \frac{Ze^2}{2\epsilon_0nh} = \frac{1 \times (1.60 \times 10^{-19} \text{ C})^2}{2 \times (8.85 \times 10^{-12} \text{ C}^2 \cdot \text{J}^{-1} \cdot \text{m}^{-1}) \times 1 \times 6.63 \times 10^{-34} \text{ J} \cdot \text{s}}$$

$$= 2.18 \times 10^6 \text{ m/s}$$

Typical nuclear velocities can be determined by measuring the vibrational frequency of diatomic molecules. For H_2 , for example, the velocity of nuclear motions is *ca.* $1 \times 10^4 \text{ m/s}$.

Thus, a molecular wave function for H_2^+ can be determined by assuming that the positions of the two nuclei are fixed and solving the Schrödinger Equation for the electron. This process is then repeated for other nuclear positions, resulting in a molecular wave function of the form:

$$\psi_{\text{mol}}(\mathbf{R}_{\text{AB}}, \mathbf{r}_A, \mathbf{r}_B, \phi) \approx \psi_{\text{el}}(\mathbf{r}_A, \mathbf{r}_B, \phi; \mathbf{R}_{\text{AB}}) \times \psi_{\text{nucl}}(\mathbf{R}_{\text{AB}})$$

Virial Theorem:

For a system of particles interacting only through potential forces, such as electrostatic forces, the averages over time of the kinetic (\mathcal{J}) and potential (\mathcal{V}) energies are related as follows:

$$\overline{\mathcal{J}} = -\frac{1}{2}\overline{\mathcal{V}} \quad (1)$$

where $\overline{\mathcal{J}}$ and $\overline{\mathcal{V}}$ are the average kinetic and potential energies, respectively. Since

$$\overline{\mathbf{E}} = \overline{\mathcal{J}} + \overline{\mathcal{V}} \quad (2)$$

then for any process that involves a change in overall system energy,

$$\Delta\overline{\mathbf{E}} = \Delta\overline{\mathcal{J}} + \Delta\overline{\mathcal{V}} \quad (3)$$

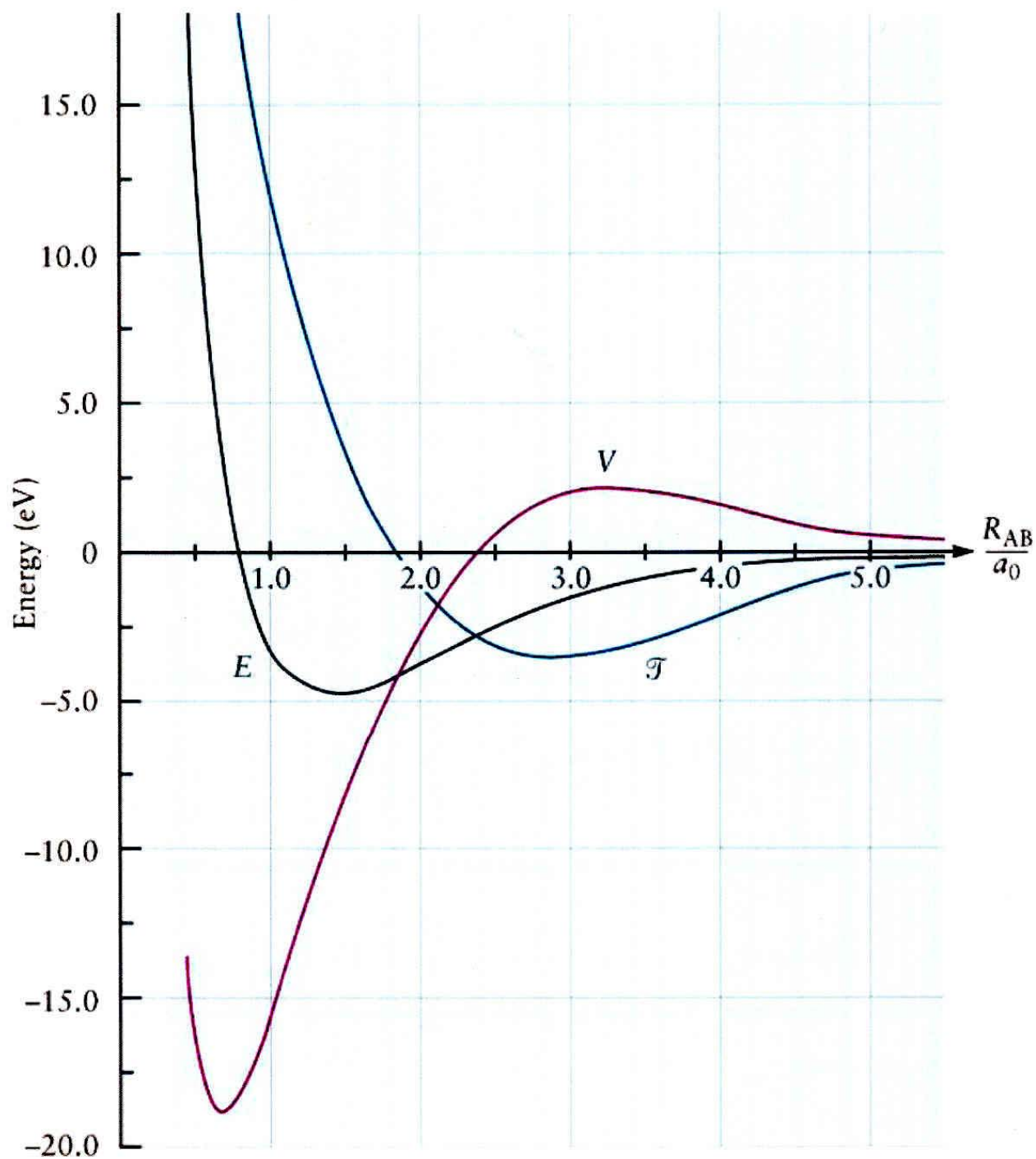
Therefore,

$$\Delta\overline{\mathbf{E}} = \frac{1}{2}\Delta\overline{\mathcal{V}} \quad (4)$$

and

$$\Delta\overline{\mathcal{J}} = -\frac{1}{2}\Delta\overline{\mathcal{V}} \quad (5)$$

Thus, according to the virial theorem (Eq. 4), the reduction in total energy has the same sign as the reduction in potential energy. Also, according to Eq. 5, the kinetic energy increases, but only by half as much as the potential energy decreases. As a result, for cases in which the potential energy makes the predominant contribution to the total energy (*e.g.*, ionic bonds), the reduction in potential energy can be considered to be the principal driving force for bond formation. However, for bonds in which both potential and kinetic energies play important roles (*e.g.*, covalent and polar covalent bonds), the driving force for bond formation is the reduction in total energy, which involves counter-balanced changes in both kinetic and potential energies.



Average values of the total (E), kinetic (T), and potential (V) energies of H₂ as a function of the internuclear distance.

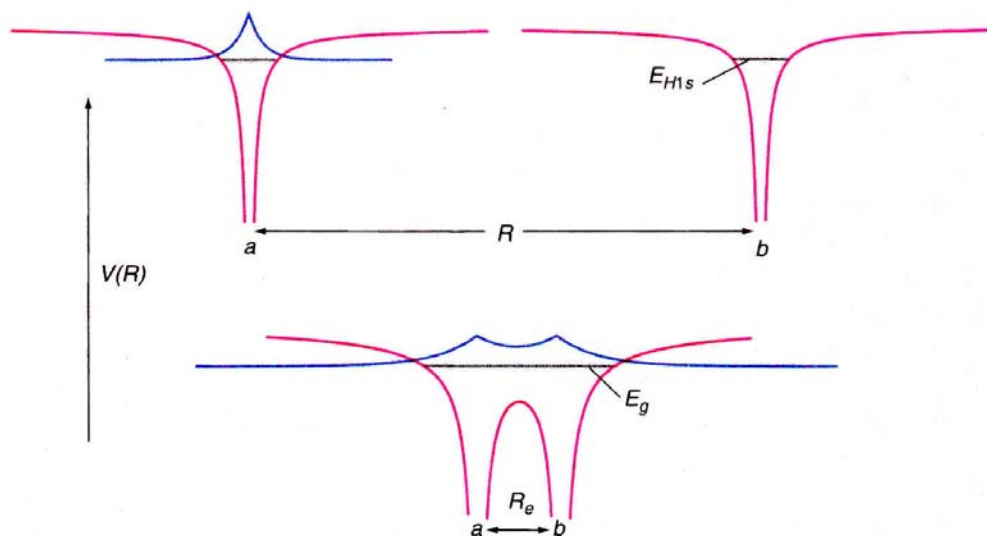


FIGURE 23.2

The potential energy of the H_2^+ molecule is shown for two different values of R (red curves). At large distances, the electron will be localized in a $1s$ orbital either on nucleus a or b . However, at the equilibrium bond length R_e , the two Coulomb potentials overlap, allowing the electron to be delocalized over the whole molecule. The blue curve represents the amplitude of the atomic (top panel) and molecular (bottom panel) wave functions, and the solid horizontal lines represent the corresponding energy eigenvalues.

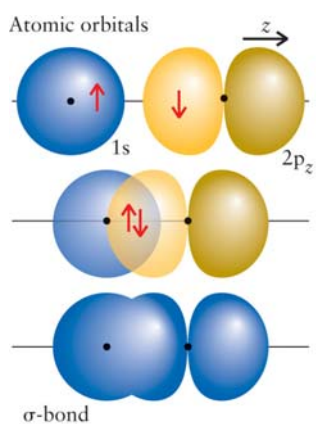


FIGURE 4.9 A σ -bond can also be formed when electrons in $1s$ - and $2p_z$ -orbitals pair (where z is the direction along the internuclear axis). The two electrons in the bond are generally found spread over the entire region of space enclosed by the boundary surface.

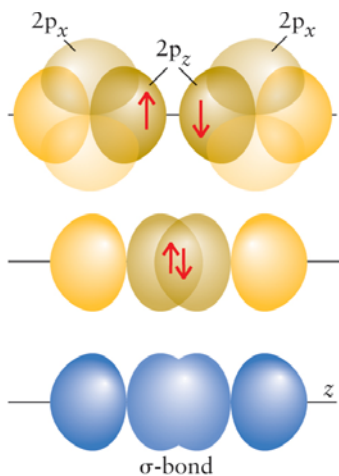


FIGURE 4.10 A σ -bond is formed by the pairing of electron spins in two $2p_z$ -orbitals on neighboring atoms. At this stage, we are ignoring the interactions of any $2p_x$ - (and $2p_y$ -) orbitals that also contain unpaired electrons, because they cannot form σ -bonds. Most of the time the bonding electron pair is found within the boundary surface shown in the bottom diagram. Notice that the nodal plane of each p_z -orbital survives in the σ -bond.

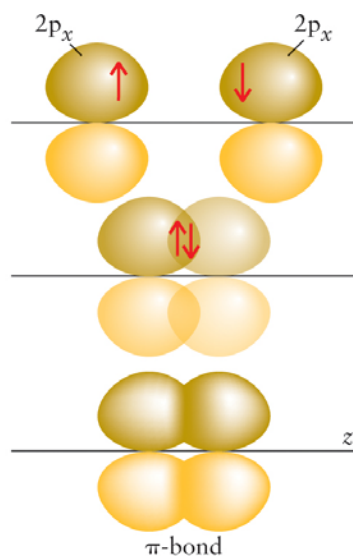


FIGURE 4.11 A π -bond is formed when electrons in two $2p$ -orbitals pair and overlap side by side. The middle diagram shows the extent of the overlap, and the bottom diagram shows the corresponding boundary surface. Even though the bond has a complicated shape, with two lobes, it is occupied by one pair of electrons and counts as one bond. In this text, π -bonds are usually colored a shade of yellow.

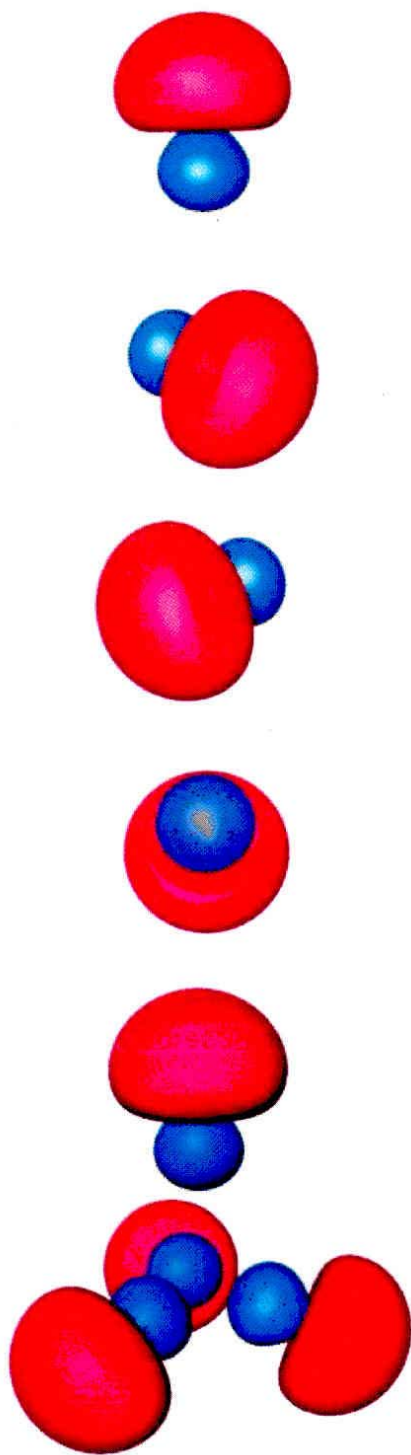


FIGURE 6.43 Shapes and relative orientations of the four sp^3 hybrid orbitals in CH_4 pointing at the corners of a tetrahedron with the carbon atom at its center. The "exploded view" at the bottom shows the tetrahedral geometry.

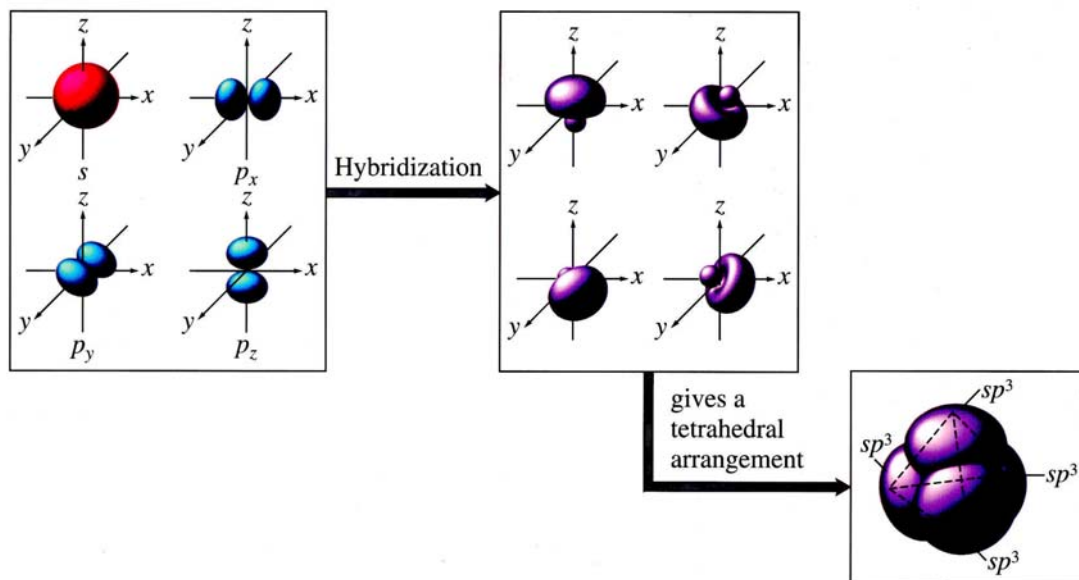


Figure 9.3
The formation of sp^3 hybrid orbitals

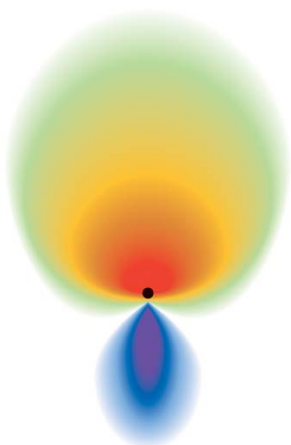


FIGURE 4.13 These contours indicate the amplitude of the sp^3 hybrid orbital wavefunction in a plane that bisects it and passes through the nucleus. The colors indicate the variation of electron density in the orbital: regions of high electron density are red and regions of low electron density are blue. Each sp^3 hybrid orbital points toward the corner of a tetrahedron.

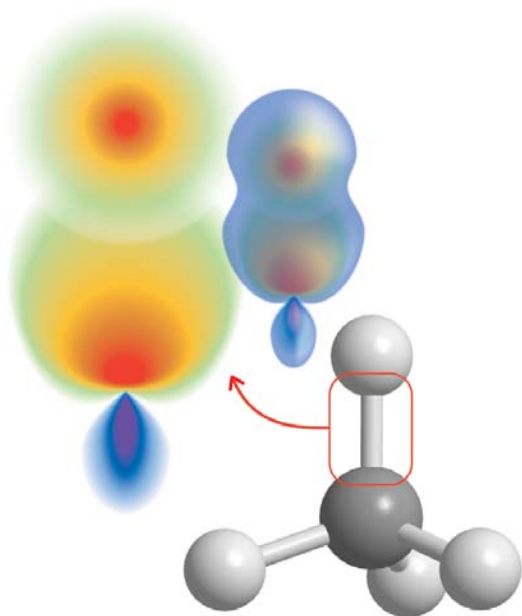


FIGURE 4.14 Each C—H bond in methane is formed by the pairing of an electron in a hydrogen 1s-orbital and an electron in one of the four sp^3 hybrid orbitals of carbon. Therefore, valence-bond theory predicts four equivalent σ -bonds in a tetrahedral arrangement, which is consistent with experimental results. The sp^3 orbital is shown in both contour form (see Fig. 4.13) and as a boundary surface.

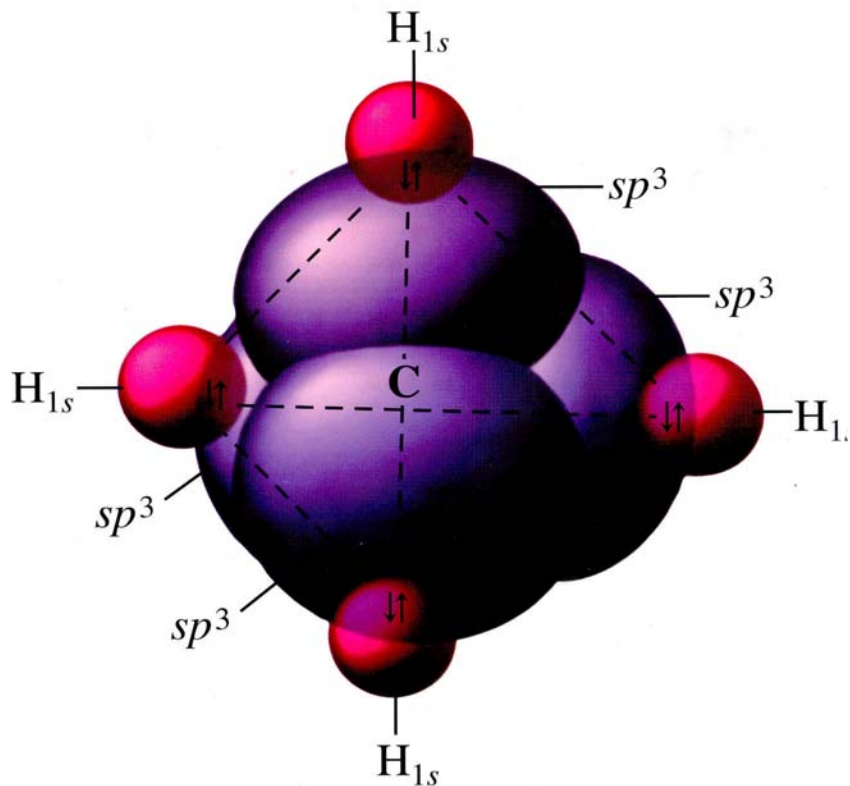


Figure 9.6
The orbitals in CH₄

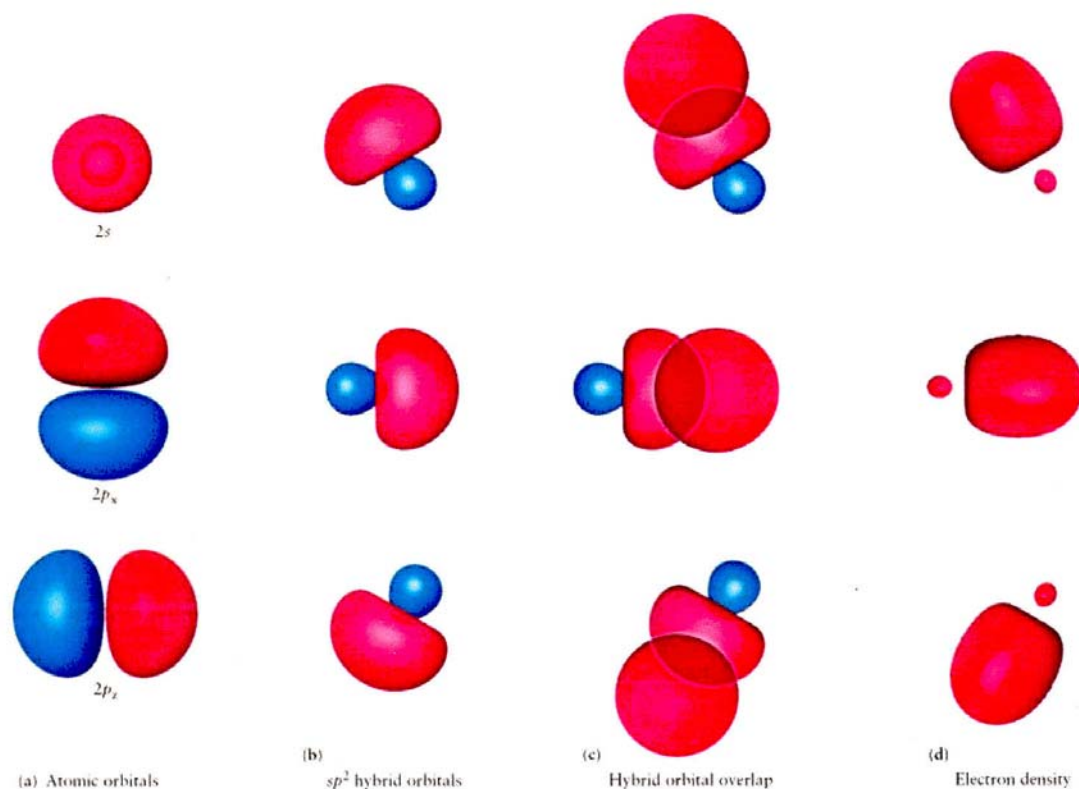


FIGURE 6.42 Formation, shapes, relative orientation, and bonding of the three sp^2 hybrid orbitals in the BH_3 molecule. (a) The $2s$, $2p_x$, and $2p_y$ atomic orbitals on a boron atom. (b) The three sp^2 hybrid orbitals on a boron atom. (c) Overlap of the sp^2 hybrid orbitals with hydrogen $1s$ orbitals to form three σ bonds in BH_3 . (d) Electron density in the three σ bonds as calculated by Generalized Valence Bond (GVB) theory.

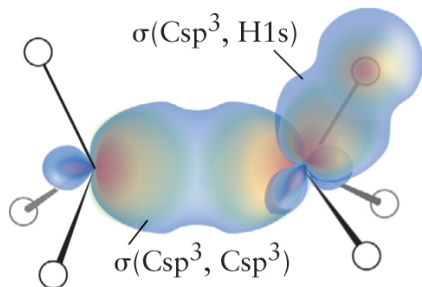


FIGURE 4.15 The valence-bond description of bonding in an ethane molecule, C_2H_6 . The boundary surfaces of only two of the bonds are shown. Each pair of neighboring atoms is linked by a σ -bond formed by the pairing of electrons in either $H1s$ -orbitals or $C2sp^3$ hybrid orbitals. All the bond angles are close to 109.5° (the tetrahedral angle).

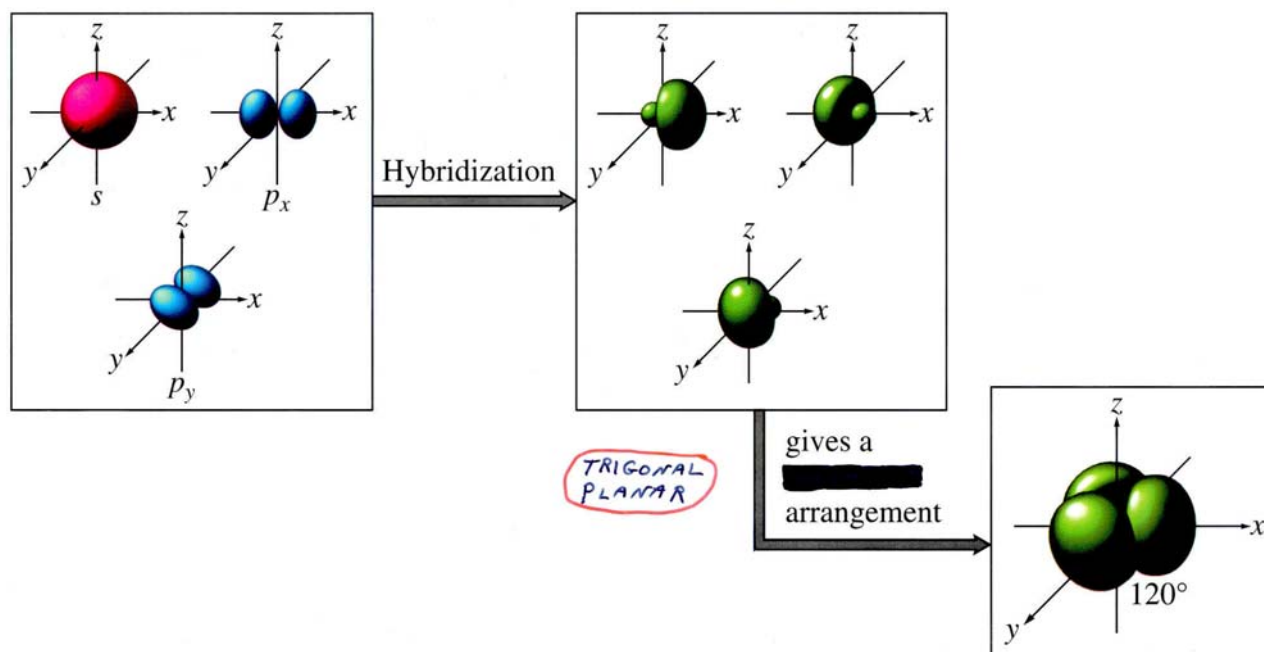


Figure 9.8
The formation of sp^2 hybrid orbitals

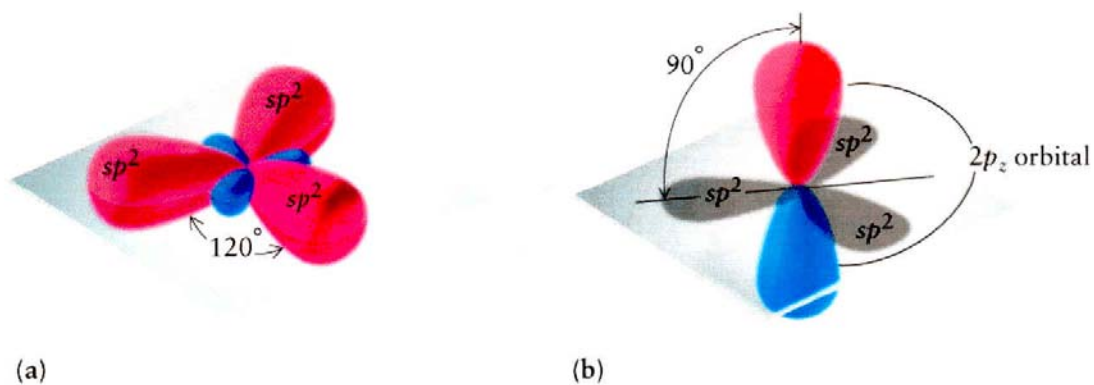


FIGURE 7.11 Sketches of sp^2 hybridized orbitals on carbon. (a) The three sp^2 hybridized orbitals are oriented in a plane with their axes at angles of 120 degrees. (b) The non-hybridized $2p$ orbital is perpendicular to the plane containing the three sp^2 hybrid orbitals.

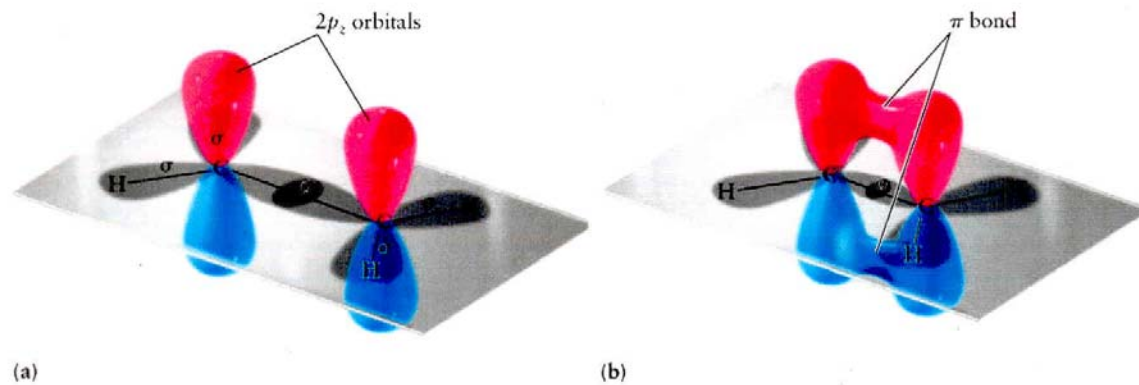


FIGURE 7.12 Bond formation in ethylene. (a) Overlap of sp^2 hybrid orbitals forms a σ bond between the carbon atoms. (b) Overlap of parallel $2p$ orbitals forms a π bond.

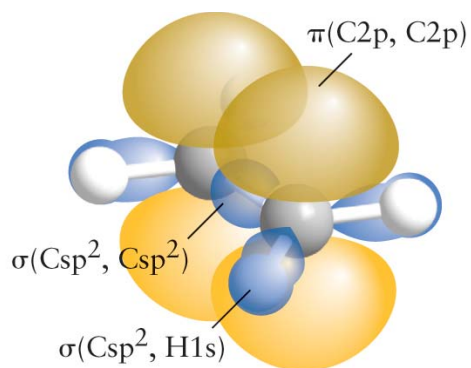


FIGURE 4.19 A view of the bonding pattern in ethene (ethylene), showing the framework of σ -bonds and the single π -bond formed by side-to-side overlap of unhybridized C2p-orbitals. The double bond is resistant to twisting because twisting would reduce the overlap between the two C2p-orbitals and weaken the π -bond. Here the bonding structure is superimposed over a ball-and-stick model.

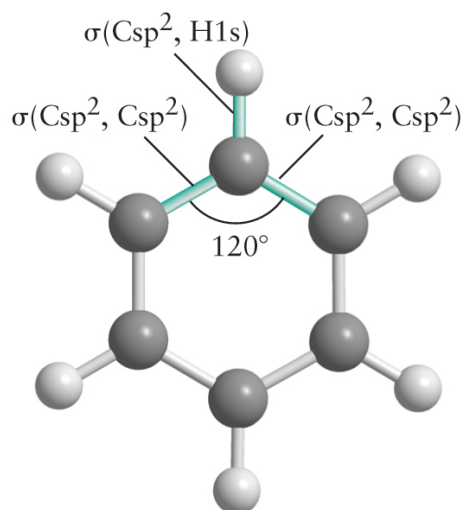


FIGURE 4.20 The framework of σ -bonds in benzene: each carbon atom is sp^2 hybridized, and the array of hybrid orbitals matches the bond angles (of 120°) in the hexagonal molecule. The bonds around only one carbon atom are labeled; all the others are the same.

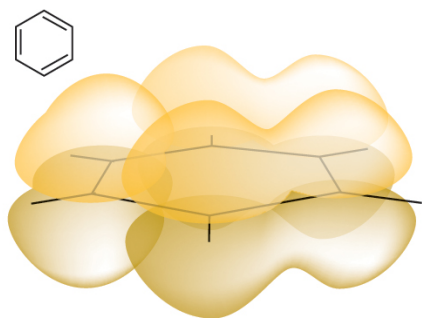


FIGURE 4.21 Unhybridized carbon 2p-orbitals can form a π -bond with either of their immediate neighbors. Two arrangements are possible, each one corresponding to a different Kekulé structure. One Kekulé structure and the corresponding π -bonds are shown here.

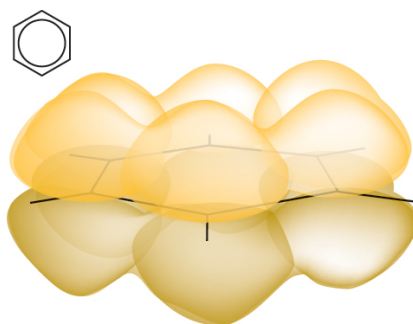


FIGURE 4.22 As a result of resonance between two structures like the one shown in Fig. 4.21 (corresponding to resonance of the two Kekulé structures), the π -electrons form a double doughnut-shaped cloud above and below the plane of the ring.

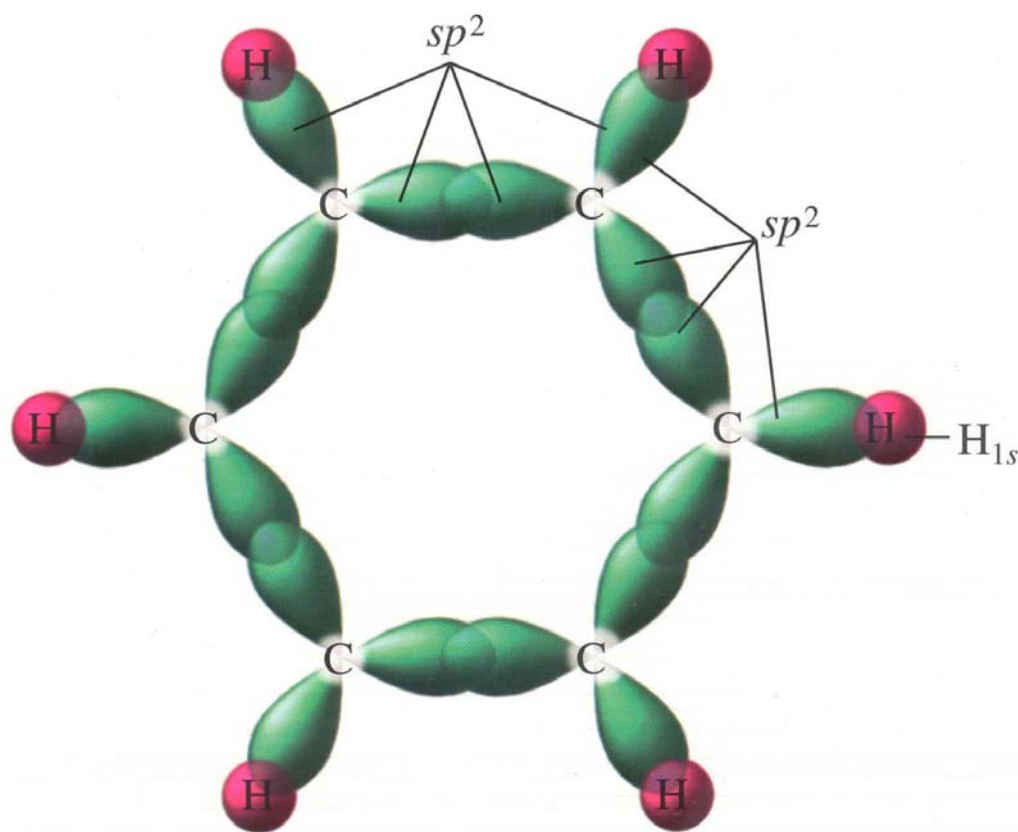


Figure 9.47
The sigma system for benzene

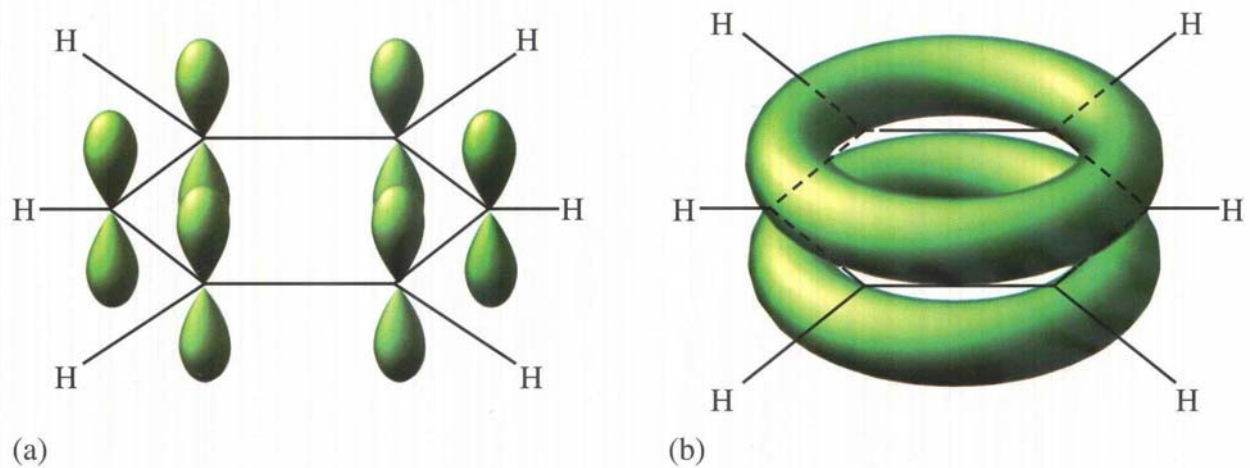


Figure 9.48
The pi system for benzene

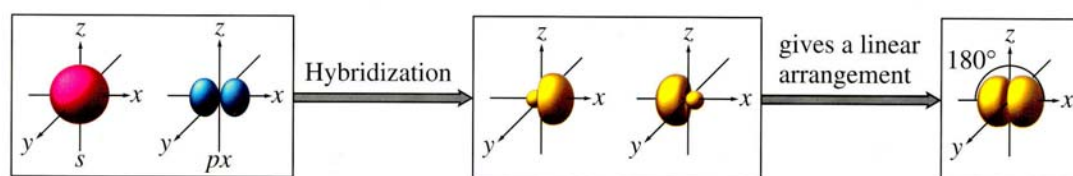


Figure 9.14
The formation of sp hybrid orbitals

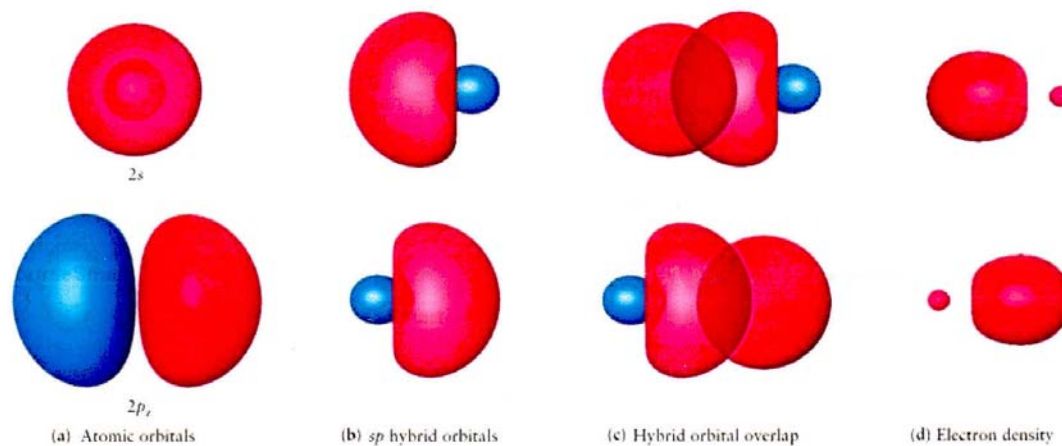


FIGURE 6.41 Formation, shapes, and bonding of the sp hybrid orbitals in the BeH_2 molecule. (a) The $2s$ and $2p$ orbitals of the Be atom. (b) The two sp hybrid orbitals formed from the $2s$ and $2p_x$ orbitals on the beryllium atom. (c) The two σ bonds that form from the overlap of the sp hybrid orbitals with the hydrogen $1s$ orbitals, making two single bonds in the BeH_2 molecule. (d) Electron density in the two σ bonds as calculated by Generalized Valence Bond (GVB) theory.

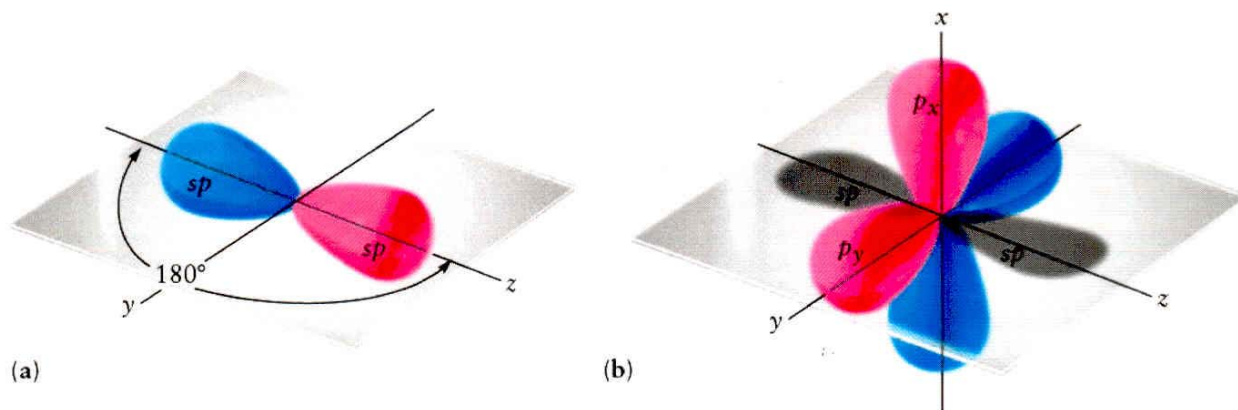


FIGURE 7.13 Sketches of sp hybridized orbitals on carbon. (a) The two sp hybridized orbitals are oriented in a plane with their axes at angles of 180 degrees. (b) Two nonhybridized $2p$ orbitals are oriented perpendicular to the axes of the two sp hybrid orbitals.

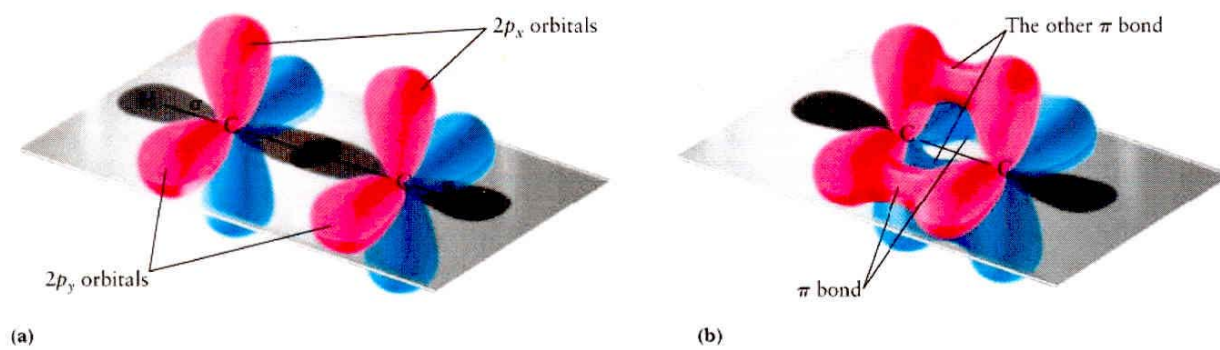


FIGURE 7.14 Bond formation in acetylene. (a) The σ bond framework and the two nonhybridized $2p$ orbitals on each carbon. (b) Overlap of two sets of parallel $2p$ orbitals forms two π bonds.

Figure 6.8: Valence Bonding in Acetylene

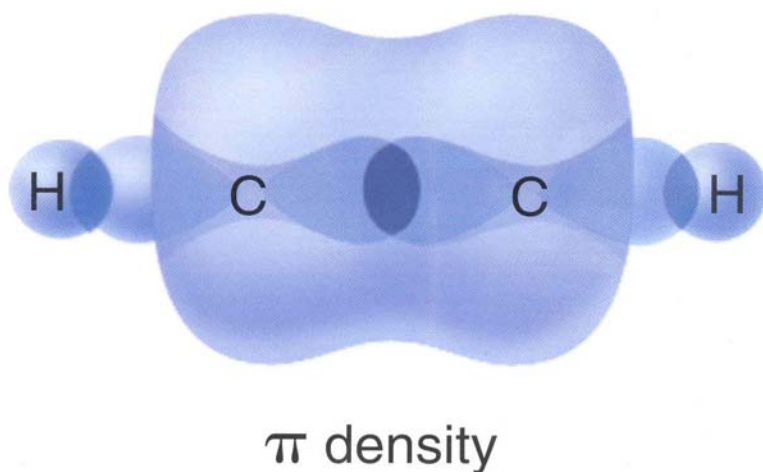
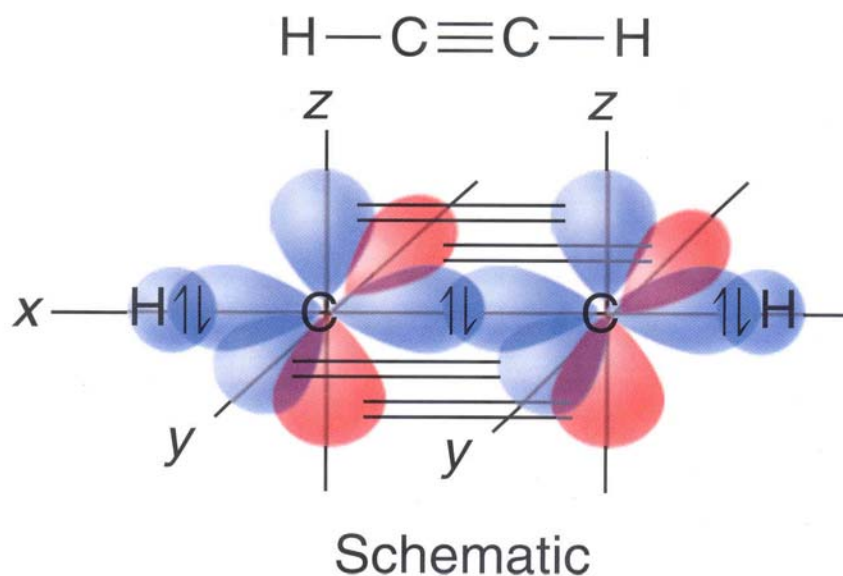


Figure 6.6

Atomic hybridization schemes for atoms A bonded to two, three, or four atoms B, with no lone pairs on A. The p orbitals used for the AB_2 and AB_3 cases depend on the choice of coordinates, as indicated at the top. The hybrids are directed along the bond axes in each case. The drawings of boundary surfaces are artificially "pointy" in order to show directionality clearly; they actually overlap in space, and the sp^3 case corresponds to a spherical overall electron density. The small negative "tails" of the hybrid orbitals are not shown. See Figure 6.5 for more realistic hybrid boundary surfaces. The hybridizations shown also apply approximately when one or more B atoms are replaced by lone pairs.

| | Linear AB_2 | Trigonal planar AB_3 | Tetrahedral AB_4 |
|---------------------------------|---------------|------------------------|--------------------|
| | | | |
| Bond angles | 180° | 120° | 109.5° |
| Atomic orbitals used in bonding | s, p_x | s, p_x, p_y | s, p_x, p_y, p_z |
| Type of hybridization | sp | sp^2 | sp^3 |
| Schematic bonding orbitals | | | |

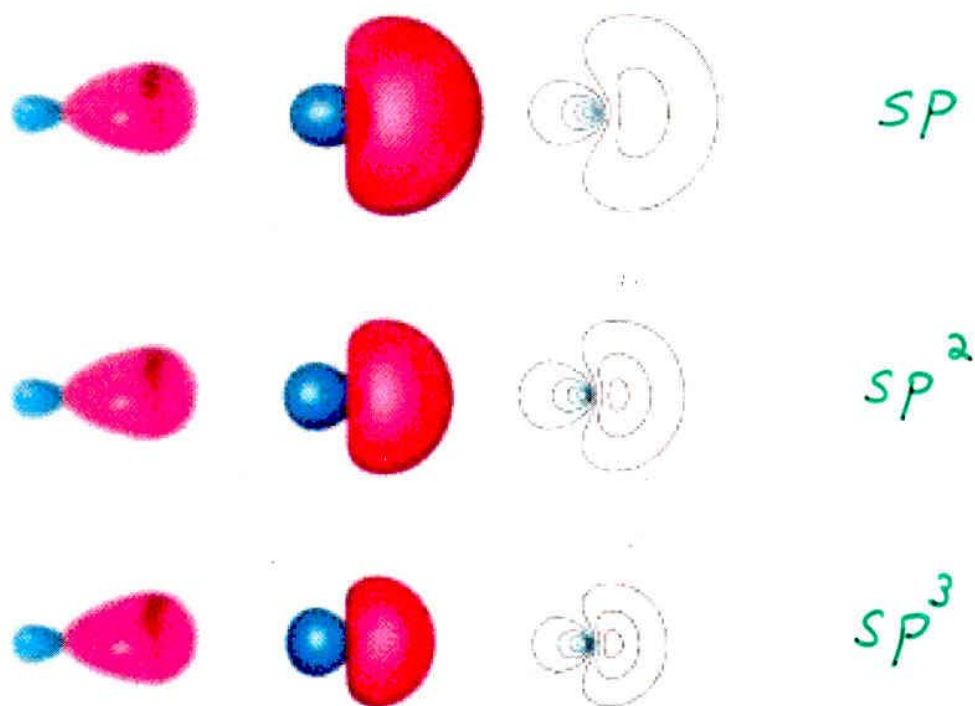
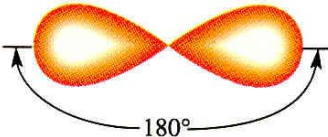
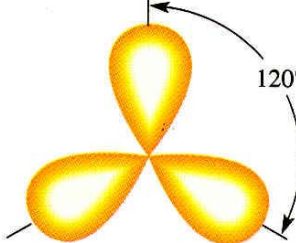
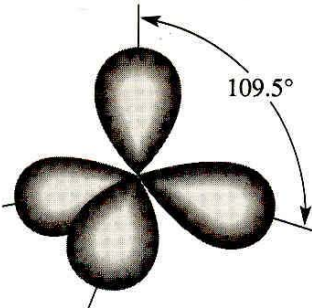
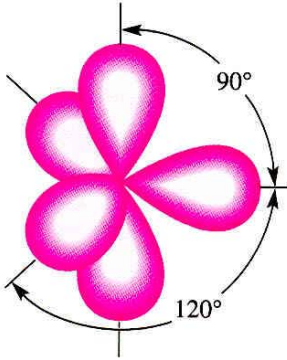
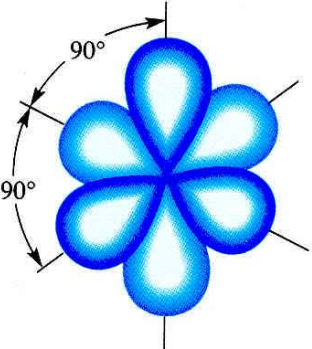
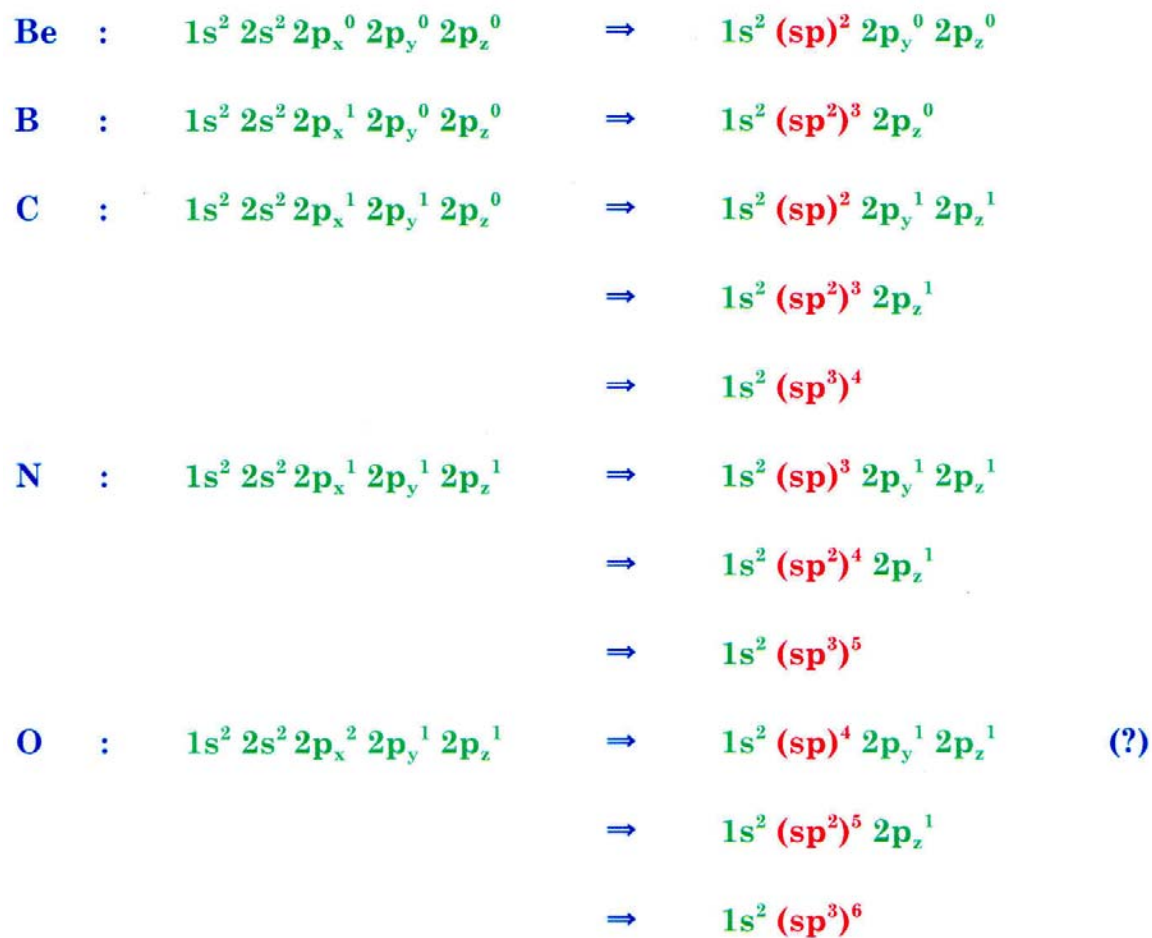


FIGURE 6.44 Exact and approximate representations of the hybrid orbital shapes. For each type of hybrid orbital shown the left column shows typical chemists' sketches, the center column shows isosurfaces, and the right column shows contour plots. The top row are the sp hybrid orbitals, the middle row are the sp^2 hybrid orbitals, and the bottom row are the sp^3 hybrid orbitals.

Hybrid Orbital Summary

| Parent Atomic Orbitals | Hybridization | Number of Hybrid Orbitals | Geometry | Shape |
|-------------------------|---------------|---------------------------|--|----------------------|
| $s + p$ | sp | 2 |  | Linear |
| $s + p + p$ | sp^2 | 3 |  | Trigonal planar |
| $s + p + p + p$ | sp^3 | 4 |  | Tetrahedral |
| $s + p + p + p + d$ | sp^3d | 5 |  | Trigonal bipyramidal |
| $s + p + p + p + d + d$ | sp^3d^2 | 6 |  | Octahedral |

Orbital "Hybridization"



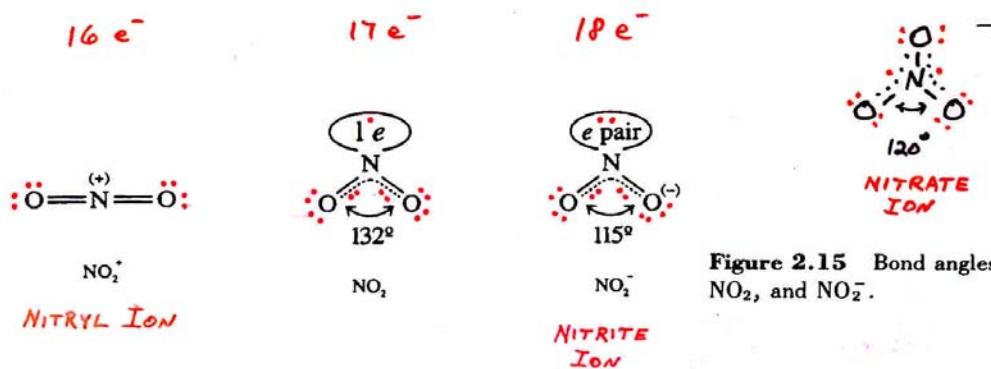


Figure 2.15 Bond angles in NO_2^+ , NO_2 , and NO_2^- .

Table 2.4 Comparison of bond angles^a

| | | | | | | |
|------------------------|----------------------|----------------------|---------------|-----------------------|--------------------|---------------|
| CH_4 | | 109.47° | | 119.9° | | 116.5° |
| CH_3F | $\angle\text{HCH}$ | 110.6° | | | | |
| CH_3Cl | $\angle\text{HCH}$ | 110.4° | | | | |
| CHF_3 | $\angle\text{FCF}$ | 108.6° | | | | |
| CHCl_3 | $\angle\text{ClCCl}$ | 111.3° | | | | |
| | | | | 114° | | 111.8° |
| | | | | 113.5° | | 107.7° |
| NH_3 | 107.2° | NF_3 | 102.3° | NCl_3 | 107.1° | |
| PH_3 | 93.2° | PF_3 | 97.7° | PCl_3 | 100.3° | |
| AsH_3 | 92.1° | AsF_3 | 95.8° | AsCl_3 | 98.9° | |
| SbH_3 | 91.6° | SbF_3 | 95.0° | SbCl_3 | 97.1° | |
| | | | | PBr_3 | 101.0° | |
| | | | | PI_3 | 102° | |
| H_2O | 104.45° | F_2O | 103.1° | F_2SO | $\angle\text{FSO}$ | 106.8° |
| H_2S | 92.1° | | | | $\angle\text{FSF}$ | 92.8° |
| H_2Se | 90.6° | | | | | |
| H_2Te | 90.2° | | | | | |

^a Data from R. J. Gillespie and I. Hargittai, *The VSEPR Model of Molecular Geometry*, Allyn and Bacon, Boston, 1991; or M. C. Favas and D. L. Kepert, *Prog. Inorg. Chem.* **1980**, *27*, 325.

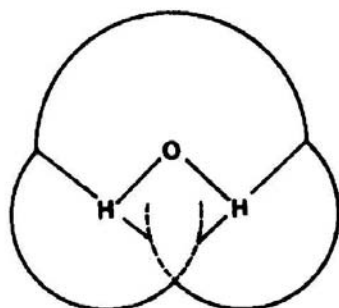


Figure 1. (left) Hypothetical water molecule with the H-O-H angle constrained to 90° . The van der Waals radii of the H atoms clearly overlap (as shown by the dotted lines); the two H atoms would penetrate each other.

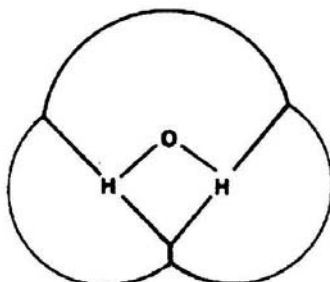


Figure 2. (center) The water molecule with the H-O-H angle set at 104.5° . The two H atoms are now in contact with slight compression.

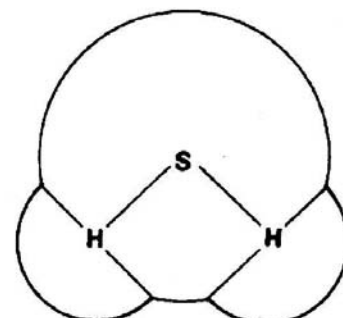
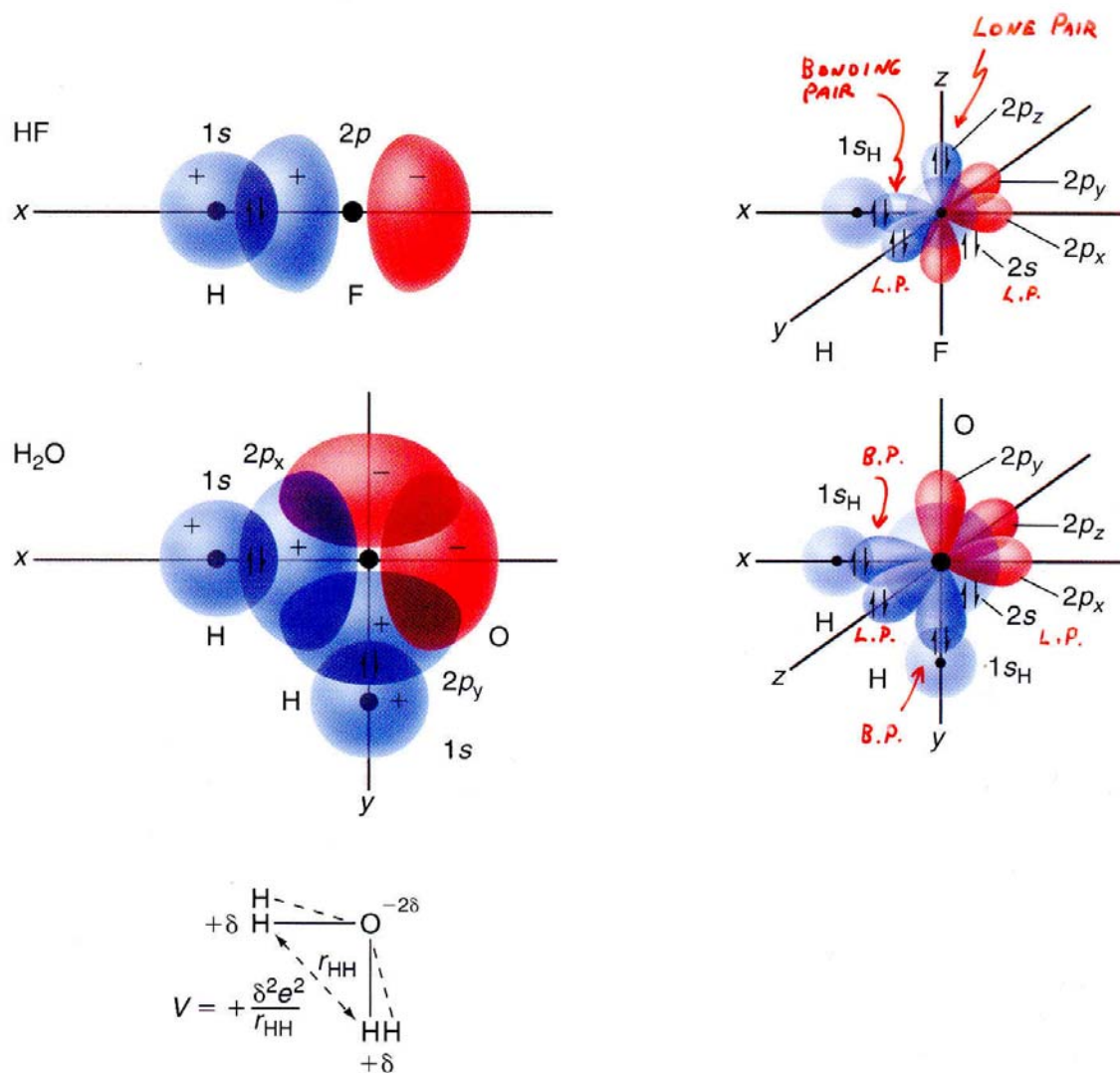


Figure 3. (right) The H_2S molecule, with the H-S-H angle of 90° . The longer S-H bond moves the H atoms apart thus eliminating the H $\cdot\cdot$ H interference which occurs in the H_2O molecule. Bond lengths are O-H, 1.0 \AA , S-H, 1.35 \AA ; van der Waals radii are O, 1.4 \AA , H, 1.1 \AA , S, 2.1 \AA .

Figure 6.3: Orbitals and Electron Pairs



VALENCE - BOND MODEL

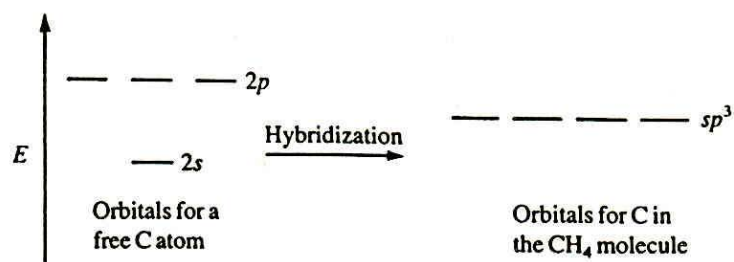


Figure 14.5

An energy-level diagram showing the formation of four sp^3 orbitals.

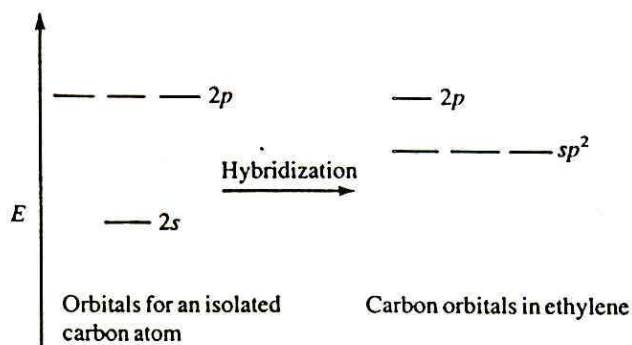


Figure 14.9

An orbital energy-level diagram for sp^2 hybridization. Note that one p orbital remains unchanged.

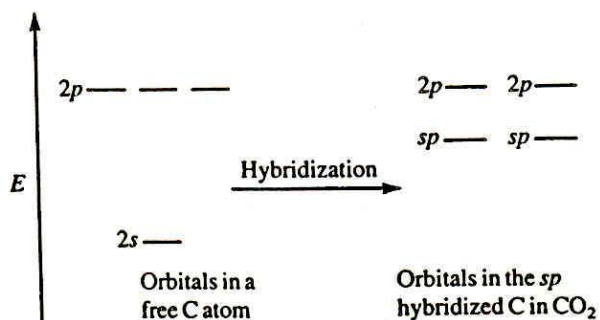


Figure 14.16

The orbital energy-level diagram for the formation of sp hybrid orbitals of carbon.

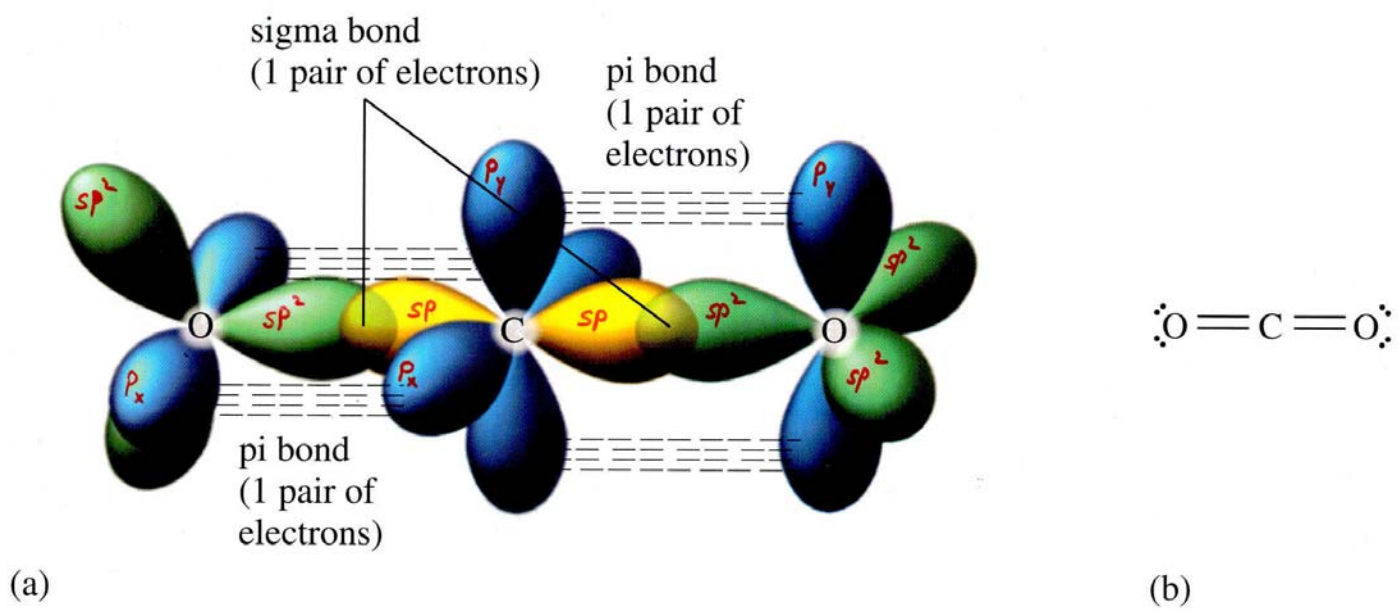
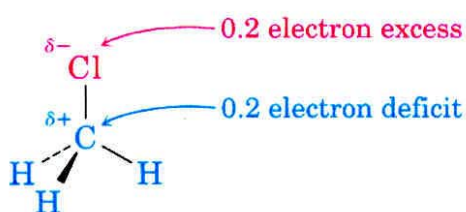


Figure 9.19
The orbitals for CO_2

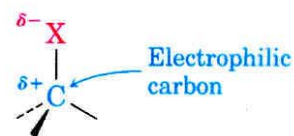
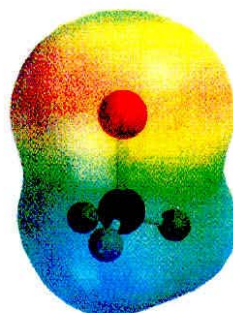
Effect of Hybridization on Dipole Moment

Because the 2s atomic orbital is lower in energy than the 2p in many-electron atoms, the electronegativity of a hybridized atom increases with increasing “s-character.” For this reason, the hybridization model predicts that an sp -hybridized carbon atom, for example, is more electronegative than an sp^3 -hybridized carbon atom.

In the chloromethane molecule, for example, experimental measurements indicate that the sp^3 -hybridized C-atom is the positive end of the C-Cl dipole, as expected based on the nominally higher electronegativity of Cl compared to C.



Chloromethane ($\mu = 1.87 \text{ D}$)



In CO, however, in which the C-atom is sp -hybridized, experimental results indicate that the C-atom is the negative end of the $\text{C}\equiv\text{O}$ dipole, despite the higher nominal electronegativity of oxygen.

Similarly, in the $\text{N}\equiv\text{C}-\text{Cl}$ molecule, which also contains an sp -hybridized C-atom, experimental results indicate that the positive end of the C-Cl dipole is on the Cl-atom, indicating that the C-atom in the cyanide group is more electronegative than the Cl-atom.